International Journal of Pharmaceutics 431 (2012) 222–229

Contents lists available at SciVerse ScienceDirect

International Journal of Pharmaceutics

journal homepage: www.elsevier.com/locate/ijpharm

Doxorubicin and MBO-asGCS oligonucleotide loaded lipid nanoparticles overcome multidrug resistance in adriamycin resistant ovarian cancer cells (NCI/ADR-RES)

Akhtar Siddiqui, Vineet Gupta, Yong-Yu Liu, Sami Nazzal*

Department of Basic Pharmaceutical Sciences, College of Pharmacy, University of Louisiana at Monroe, Monroe, LA 71209-0497, United States

ARTICLE INFO

Article history:
Received 21 December 2011
Received in revised form 11 April 2012
Accepted 19 April 2012
Available online 25 April 2012

Keywords:
Oligonucleotide
Solid lipid nanoparticles
Drug delivery
Gene delivery
Multidrug resistance

ABSTRACT

The objective of this study was to increase the potency of doxorubicin against adriamycin-resistant NCI/ADR-RES cells by concurrent treatment with doxorubicin and MBO-asGCS loaded solid-lipid nanoparticles (SLN). Loading doxorubicin as ion-pair complex with deoxytaurocholate into cationic and neutral SLN was investigated. Fast release and poor entrapment were observed in cationic nanoparticles, which were corrected by entrapping the complex in neutral polyoxyethylene (20) stearyl ether (Brij® 78)/VitE-TPGS nanoparticles. Slow doxorubicin release confirmed the influence of charge and electrolytes on the dissociation of ion-pair complexes. To evaluate antitumor activity, NCI/ADR-RES cells were treated with separate SLN: one loaded with doxorubicin and another carrying MBO-asGCS oligonucleotide. The viability of cells treated with 5 μM doxorubicin was reduced to 17.2% whereas viability was reduced to 2.5% for cells treated with both 5 μM doxorubicin SLN and 100 nM MBO-asGCS SLN. This suggested enhanced apoptosis due to sensitization and effective intracellular delivery of MBO-asGCS and doxorubicin by SLN.

1. Introduction

Development of resistance to chemotherapy, wherein drugs elicit suboptimal response to their previously effective doses in cancer, is one of the major challenges to successful chemotherapy (Choi, 2005; Gottesman, 2002; van Den Elsen et al., 1999). A major mechanism by which cells reduce the intracellular effectiveness of cytotoxic drugs is by overexpressing either P-glycoprotein (P-gp) or glucosylceramide synthase (GCS) (Liu et al., 2010; Lucci et al., 1999; Pérez-Sayáns et al., 2010; Ye et al., 2008). P-gp is an efflux transporter whereas GCS is an enzyme that modifies the efficacy of the internalized drug by modulating intracellular levels of ceramide.

The role of glycolipids in imparting multidrug resistance has only relatively recently been identified (Cabot et al., 1999; Gouaze et al., 2004; Lucci et al., 1999; Norris-Cervetto et al., 2004). Ceramide is a central glycolipid that dictates cellular fate of anticancer drugs (Gouaze-Andersson and Cabot, 2006b; Gouaze et al., 2005; Liu et al., 1999, 2000, 2001). Increase in the intracellular levels of ceramide was shown to induce apoptosis, whereas its conversion to glucosylceramide by GCS enhances cell proliferation and increases cancer resistance to chemotherapeutic agents (Gouaze et al., 2004; Liu et al., 1999). Glucosylceramide has also been implicated in the formation of membrane lipid rafts, which provide a venue for the expression of membrane-bound receptors and transporters (Gouaze-Andersson and Cabot, 2006a; Li et al., 2006; van Meer et al., 2003). Enhanced numbers of lipid rafts in the membrane increases the expression of receptor and transporters, including P-gp, leading to signal amplification or to enhanced efflux of intracellular drugs (Bacso et al., 2004).

In order to overcome drug resistance, P-gp inhibitors and formulation components known to inhibit P-gp are commonly used. P-gp inhibitors, however, have been shown to alter the pharmacokinetic and biodistribution properties of anticancer drugs (Dong et al., 2009; Wong et al., 2006a). Alternatively, colloidal delivery systems such as liposomes, niosomes, solid lipid nanoparticles, polymer-lipid hybrid nanoparticles, and micelles may overcome the resistance of cancer cells to chemotherapy by (a) enhancing drug accumulation through internalization by endocytosis, (b) partially inhibiting P-gp gene expression, (c) modulating caspase-dependent apoptotic signaling pathways, and (d) depleting ATP (Dong et al., 2009; Wong et al., 2006b). This approach, however, lacks any control over the expression of glucosylceramide synthase, which could mitigate the effectiveness of the internalized drugs. Down regulating the expression of GCS with an antisense oligonucleotide is expected to enhance the effectiveness of the internalized drugs (Patwardhan et al., 2009). The sensitizing

* Corresponding author at: Department of Basic Pharmaceutical Sciences, College of Pharmacy, University of Louisiana at Monroe, 1800 Bienville Drive, Monroe, LA 71201, United States. Tel.: +1 318 342 1726; fax: +1 318 342 1737.
E-mail address: nazzal@ulm.edu (S. Nazzal).

0378-5173/$ – see front matter © 2012 Elsevier B.V. All rights reserved.
http://dx.doi.org/10.1016/j.ijpharm.2012.04.050

effect of mixed-backbone GCS antisense oligonucleotides (MBO-asGCS) in NCI/ADR-RES human ovarian cancer cells was previously reported by our group (Liu et al., 2004).

Our previous studies with solid lipid nanoparticles (SLN) loaded with MBO-asGCS also demonstrated that MBO loaded nanoparticles sensitized the resistant NCI/ADR-RES cells to free doxorubicin in the media (Siddiqui et al., 2010). In these preliminary studies, however, doxorubicin was given in a solution form. This approach, however, may not be suitable for *in vivo* applications because doxorubicin in solution would produce the same dose-dependent cardiotoxicity as observed with treating non-resistant tumors. Therefore, entrapping doxorubicin in SLN may reduce its accessibility to the cardiac tissue (Saltiel and McGuire, 1983). Furthermore, its entrapment in lipid nanoparticles has been reported to lower the IC_{50} of the drug against adriamycin-resistant (P388/ADR) murine leukemia cells (2009), which was attributed to the ability of nanoparticles to bypass the P-gp efflux transporter on the cell membrane (Wong et al., 2006c, 2007). To complement earlier studies on doxorubicin-loaded nanoparticles, the overall objective of the present study was to investigate whether the potency of doxorubicin nanoparticles against adriamycin-resistant (NCI/ADR-RES) ovarian cancer cells *in vitro* may be enhanced by concurrently treating the cells with MBO-asGCS-loaded lipid nanoparticles. More specifically, the first objective of this study was to prepare, characterize and optimize the process for preparing lipophilic doxorubicin ion pair complexes. The second objective was to investigate whether the ion pair complexes could be incorporated into stearyl alcohol based solid-lipid nanoparticles (SA-SLN), and to characterize the nanoparticles in terms of size, zeta potential, stability and effects on cell viability. The third objective was to evaluate the potency of the concurrent treatment with doxorubicin ion pair loaded SLN and MBO-asGCS loaded SLN against Adriamycin resistant NCI/ADR RES human ovarian cells.

2. Materials and methods

2.1. Materials

Stearyl alcohol and cetyltrimethylammonium bromide (CTAB) were purchased from TCI (Portland, OR). Ceramide VI was a generous gift from Evonik (Norwalk, CT). Fetal bovine serum was purchased from Hyclone (Logan, UT). Tweens®60 and Brij® 78 were provided by UniQuema (New Castle, DE). Sodium deoxytaurocholate, D-(+)-trehalose and ingredients used for phosphate buffer preparation were obtained from Sigma (St. Louis, MO). Doxorubicin HCl was purchased from NetQem (Research Triangle Park, NC). Vitamin E TPGS (vitamin E d-alpha tocopheryl polyethylene glycol succinate) was supplied by Eastman (Angelsey, UK). Mannitol was generously gifted by SPI pharma (Wilmington, DE), and sucrose was obtained from Cargill (Cedar Rapids, IA). Purified water for the dispersion was obtained from a Nanopure Ultra® water system.

2.2. Preparation of doxorubicin ion-pair complex

The doxorubicin deoxytaurocholate ion-pair complex was prepared as reported by Ma et al. (2009). Briefly, aqueous solutions of sodium deoxytaurocholate (DTC) and doxorubicin (Dox) were mixed at molar ratios of sodium deoxytaurocholate to doxorubicin ranging from 2:1 to 16:1, and centrifuged at 3075 × *g* for 1 h (Centrific™ Centrifuge, Model 225, Pittsburg, PA). The precipitate thus formed as a result of complexation was recovered after drying under vacuum. Furthermore, the effects of varying centrifugation speed from 417 to 3075 × *g*, and centrifugation time (15, 30, 60, 90, 120, and 150 min) on yield size were evaluated. In all cases, the amount of free doxorubicin in the supernatant after centrifugation was measured by UV analysis at 480 nm (λ_{max}). No interference due to free DTC in water on UV absorbance was observed. The percentage of DTC-Dox ion pair complex was calculated by applying the following equation:

$$\%\text{Doxorubicin Complex} = \frac{(\text{Total doxorubicin added} - \text{Doxorubicin in supernatant})}{\text{Total doxorubicin added}} \times 100$$

2.3. Preparation of SLN

SLN were prepared by a modified microemulsion method combining shear and ultrasonic homogenization techniques. Four types of SLN nanoparticles (SLN1-4, Table 1) were prepared. In SLN 1, 2, and 3, Stearyl alcohol at a concentration of either 0.5% or 0.25% (w/w) was first heated to 90 °C. Then 0.18% (w/v) DTC-Dox ion-pair complex was dissolved in an adequate quantity of ethyl alcohol. The ion pair solution was added to the molten stearyl alcohol, and the remaining ethyl alcohol was evaporated under a stream of nitrogen gas. A preheated aqueous solution of CTAB or CTAB/ceramide VI or CTAB/ceramide VI/polysorbate 60 blend was then transferred to the dried solid. The liquid dispersion thus formed was homogenized for 5 min at 25,000 rpm, using an UltraTurrax® T10 homogenizer (IKA, Wilmington, NC). Thereafter, the crude o/w emulsion was ultrasonicated for 0, 2.5, 5, 7.5, and 10 min at 40% power and 60% pulse frequency using a probe sonicator (Model 150 V/T, Biologics, Inc., Manassas, VA). SLN were formed by cooling the emulsion at ambient conditions to room temperature. SLN4 was prepared from a blend of stearyl alcohol/Brij® 78/Vitamin E d-alpha tocopheryl polyethylene glycol succinate (Vit. E TPGS) (Table 1) at a weight ratio of 1:1.2:1.6. The lipid and surfactant mixture were allowed to melt, and an ethanolic solution of the DTC-DOX ion pair complex was added. The ethyl alcohol was then evaporated under a stream of nitrogen gas. Preheated water was added to the solid mixture of lipid DTC-Dox ion-pair complex. The formulation was shear homogenized for 1 min at 11,500 rpm using UltraTurrax® T10. The mixture was then sonicated for 2.5 min as described above, and doxorubicin-loaded SLN were formed by cooling the formulation under ambient conditions to room temperature.

2.4. Determination of entrapment efficiency (EE)

Entrapment of DTC-Dox ion pair complex was determined by an indirect method using Amicon Ultra Centrifugation filters (MW cut-off 30,000) (Millipore, MA). An adequate volume of doxorubicin-loaded SLN (1 mL) was added to the tube, which was then centrifuged at 3075 × *g* for 15 min at room temperature. The filtrate was collected and taken as free drug. The UV absorbance of the filtrate at λ_{max} 480 nm was used to estimate the amount of free drug. In order to calculate the amount of free doxorubicin in the water, calibration curve was generated using known quantity of doxorubicin dissolved in water. The equation fitted to the curve for a particular range of doxorubicin was used for estimating the quantity of the doxorubicin by substituting the absorbance value in the equation. The EE of doxorubicin in SLN was obtained as the ratio of actual and theoretical loading as follows:

$$\text{EE}(\%) = \frac{(\text{Total amount of drug added} - \text{Amount of free drug})}{\text{Total Amount of drug added}} \times 100$$

Table 1
Effect of nanoparticles composition and sonication time on particle size, zeta potential and entrapment efficiency of doxorubicin ion-pair complex (0.18% w/v).

SLN	Composition	Sonication time (min)	Particle size (nm)	Zeta potential (mV)	EE (%)
SLN1	SA:CTAB 2:1 (drug loaded)	0	374.0 ± 37.3	50.3 ± 1.5	42.3 ± 0.9
		2.5	247.0 ± 3.5	44.1 ± 0.7	36.5 ± 2.6
		5	264.0 ± 3.8	41.0 ± 0.5	34.5 ± 1.1
		7.5	257.0 ± 1.3	39.3 ± 1.2	32.2 ± 0.3
		10	250.2 ± 1.5	38.7 ± 0.3	33.0 ± 1.1
	(Drug free)	10	167.0 ± 1.6	39.3 ± 0.2	na
SLN2	SA:CTAB:Ceramide VI 1:1:1(drug loaded)	0	89.0 ± 1.4	42.0 ± 2.6	<5
		2.5	101.2 ± 1.1	35.7 ± 0.6	<5
		5	75.3 ± 0.4	37.1 ± 2.8	<5
		7.5	63.0 ± 0.5	32.4 ± 1.8	<5
		10	57.0 ± 0.6	34.4 ± 1.3	<5
	(Drug free)	10	74.6 ± 1.2	38.8 ± 2.3	na
SLN3	SA:CTAB:Ceramide VI:Polysorbate 60	0	209.5 ± 4	36.0 ± 0.4	35.0 ± 2.2
	1:1:0.5:0.5(drug loaded)	2.5	153.4 ± 3.6	34.2 ± 1.4	35.1 ± 2.7
		5	146.1 ± 0.9	33.0 ± 0.7	30.2 ± 2.8
		7.5	114.4 ± 1.6	35.4 ± 0.3	31.3 ± 2.3
		10	105.2 ± 1.4	35.3 ± 0.9	23.6 ± 0.9
	(Drug free)	10	109.1 ± 0.9	nd	na
SLN4	SA:Brij®78:Vit E TPGS: 1:1.2:1.6 (drug Loaded)	0	165.6 ± 0.9	(−)5.6 ± 0.3	93.5 ± 0.4
		2.5	129.0 ± 0.2	(−)5.6 ± 0.8	95.1 ± 0.3
		5	163.4 ± 1.6	(−)6.2 ± 0.4	94.2 ± 0.4
		10	233.4 ± 1.1	(−)6.0 ± 0.3	94.8 ± 0.3
	(Drug free)	2.5	158.2 ± 1.6	nd	na

na = not applicable and nd = not determined.

2.5. Particle size and zeta potential measurement

The mean particle size of a given SLN preparation was measured by photon correlation spectroscopy using a Nicomp™380 ZLS (Particle Sizing System, Port Richey, FL). The size was recorded at 25 °C by scattering light at an angle of 90° for 90 s, with viscosity and dielectric constant of the medium set to 1.33 and 78.5, respectively. As recommended by the manufacturer, SLN formulations were diluted with Nanopure water in order to minimize multiple-particle scattering and to achieve an optimal scattering intensity of 300 kHz. The intensity-weighted mean diameter of the particles was calculated based on the Stokes–Einstein law by curve fitting of the correlation function (Nicomp ZLS User Manual, release date 08/03). The change in particle size with time at room temperature was taken as an index of SLN stability. The zeta potential of the SLN was measured using the same instrument (Nicomp™380 ZLS) under zeta mode. The sample was diluted with Nanopure water, and Zeta potential was measured by the Helmholz–Smoluchowsky equation as follows:

$$\xi = \frac{\eta\mu}{\varepsilon}$$

where ξ, η, μ, and ε are mean zeta-potential, viscosity, electrophoretic mobility and dielectric constant, respectively (Nicomp ZLS User Manual, release date 08/03).

2.6. Lyophilization of SLN

Lyophilization was performed on SLN dispersions diluted with cryoprotectant solutions containing trehalose, mannitol, or sucrose at concentration ranging from 0% to 20% (w/v). Samples frozen for 24 h at −80 °C were lyophilized at −55 °C at a pressure of 1.65 Torr for 20 h (Labconco, Free zone 6, Kansas city, MO). The obtained SLN lyophilizate was stored in tightly closed glass vials at room temperature until used. Samples reconstituted with deionized distilled water were analyzed for particle size as described in Section 2.5.

2.7. In vitro drug release

In vitro release studies were performed 24 h after SLNs were prepared. Doxorubicin-loaded SLN (4 mL) was placed in a dialysis tube (Spectra/por® dialysis tubes, MWCO 25,000, Spectrum Labs, Rancho Dominguez, CA). Both ends of the tube were sealed and carefully checked for possible leakage. Dialysis tube containing the doxorubicin-SLN suspension was placed in 200 mL of water or phosphate buffered medium at pH 7.4 and 6.8. The media along with the dialysis bag containing doxorubicin loaded SLN were stirred in the dark using magnetic bar. Samples (2 mL) were withdrawn from the dissolution medium after 1, 2, 4, 8, 16, 32 and 48 h, and replaced with the same amount of fresh medium. The amount of doxorubicin released was quantified by the UV spectrophotometric method described above.

2.8. Preparation of MBO-asGCS SLN complexes

MBO-asGCS SLN complex was prepared as described by Siddiqui et al. (2010). Briefly, SLN2 were first sterilized. After filtration, MBO-asGCS at various ratios of CTAB to MBO-asGCS ranging from 0.62:1 to 25:1 (w/w) was added to the aqueous SLN dispersion and the mixtures were immediately vortexed for 20 s. After vortexing, the formulations were allowed to stand for half an hour at room temperature to allow the MBO-asGCS to bind with the SLN.

2.9. Cell culture and reagents

Drug-resistant NCI/ADR-RES human ovarian cancer cells were kindly provided by Dr. Kenneth Cowan (UNMC Eppley Cancer Center, Omaha, NE) and Dr. Merrill Goldsmith (National Cancer Institute, Bethesda, MD). Cells were cultured in RPMI-1640 medium (with 10% fetal bovine serum, 100 units/mL penicillin, 100 μg/mL streptomycin, 584 mg/liter L-glutamine) and maintained in an incubator humidified with 95% air and 5% CO_2 at 37 °C. The selection of this cell line was based on previous studies in which the effect of MBO-asGCS was examined in adriamycin resistant and sensitive cells (NCI/ADR-RES, MCF-7, EMT6/AR1, and EMT6). No significant reduction in the level of GCS was found when healthy cells

Table 2
Effect of mixing various molar ratios of sodium deoxytaurocholate (DTC) and doxorubicin (DOX) on percent doxorubicin complex.

DTC to DOX (Molar ratio)	% Dox complexed
2	49.4
3	60.2
4	58.0
8	55.0
16	38.0

were treated with the oligonucleotide, whereas in resistant cells, oligonucleotide significantly reduced the level of GCS. Nonetheless, uptake of MBO-asGCS in adriamycin resistant and sensitive cells (NCI/ADR-RES and MCF-7) was found to be similar (Patwardhan et al., 2009)

2.10. Cell viability assay

This assay was performed to screen for non-specific toxicity of the formulations to cells and to investigate the viability of the cells treated with MBO-asGCS SLN complex in the presence or absence of doxorubicin loaded SLN. Cell viability was determined by quantitating ATP as an indicator of live cells, using the CellTiter-Glo® luminescent cell viability assay kit (Promega, Madison, WI) as described by Patwardhan et al. (2009). Briefly, cells (4000 cells/well) were plated in 96-well plates with 10% FBS RPMI-1640 medium overnight. Cells were either treated with drug or oligonucleotide-free SLN, doxorubicin-loaded SLN, oligonucleotide-loaded SLN (100 nM), or concurrent treatment of doxorubicin and oligonucleotide-loaded SLN. Cells treated with Lipofectamine™ 2000 (Invitrogen, Carlsbad, CA), or Lipofectamine®2000 plus MBO-asGCS, were used as controls. A separate set of studies were carried out in which doxorubicin (5 μM) was added as a free hydrochloride salt solution to all treatments. After treatment, cells were kept for 72 h after which cell viability was determined by measuring their luminescence after incubation with the CellTiter-Glo® reagent in a Synergy HT microplate reader (BioTek, Winnooski, VT).

2.11. Statistical analysis

Data were analyzed by ANOVA. Linear contrast was used whenever necessary to distinguish the differences in mean particle size and zeta potential. The Bonferroni method of multiple comparisons was carried out to help interpret cell viability data. The differences were considered significant if $p < 0.05$.

3. Results

3.1. Preparation and characterization of DTC-Dox ion pair complex

An ion pair complex of DTC-Dox was prepared at various molar ratios as described in the methods section. The percent of doxorubicin complexed at DTC:doxorubicin ratios of 2:1, 3:1, 4:1, 8:1, and 16:1 were 49%, 60%, 58%, 55% and 38%, respectively (Table 2). Dried complexes were further characterized by FTIR (data not shown), which did not reveal any detectable changes in spectra in comparison to pure doxorubicin and sodium DTC, or their physical mixture. To determine the exact stoichiometric ratio of DTC:doxorubicin, elemental analysis on the complex that was recovered at the optimal (3:1) ratio was performed at Atlantic Microlab, Inc. (Norcross, GA). Based on the elemental analysis data (not shown) it was concluded that doxorubicin in the complex formed a 1:1 ion pair with DTC.

Table 3A
Effect of complex processing conditions on the yield size. Effect of centrifugation time on recovery of doxorubicin as ion pair complex at a centrifugation speed of 4750 rpm (3075 × *g*). The data reported are mean ± standard deviation of $n = 3$ replicates. Result obtained for centrifugation time 15–45 min were significantly different (p-value <0.05). Statistical analysis was carried out by linear contrast where p-value <0.05 was considered statistically different.

Centrifugation time (min)	% Dox complexed
15	43.2 ± 3.1
30	63.7 ± 0.3
60	79.0 ± 0.3
90	87.3 ± 0.1
120	87.6 ± 0.2
150	88.0 ± 0.1

In order to maximize the yield of the ion pair complex, centrifugation time, and centrifugation speed were optimized. Mixtures were centrifuged for 15, 30, 60, 90, 120 or 150 min. The percentage of doxorubicin complexed initially increased significantly with an increase in centrifugation time and reached a plateau after 90 min (Table 3A). While keeping a constant centrifugation time at 90 min, the fraction of doxorubicin recovered as ion pair increased as the centrifugation speed increased (Table 3B).

3.2. Entrapment of DTC-Dox ion pair complex in SLN

Drug-free and DTC-Dox complex-loaded cationic SLN1 and SLN2 (Table 1) were initially prepared. Doxorubicin loading into SLN1 brought about significant increases in mean particle size. A maximum of approximately 43% of doxorubicin was entrapped, which decreased with an increase in sonication time during nanoparticle preparation. In comparison, less than 5% of doxorubicin was entrapped in SLN2 regardless of sonication time (Table 1). This may be attributed to the partial substitution of CTAB with ceramide VI, which enhanced lipid packing density and thereby significantly reduced particle size. Tight packing of lipid after re-crystallization may be responsible for the expulsion of the ion-pair complex and significantly lower EE when compared with SLN1 (Müller et al., 2000).

To improve entrapment efficiency, polysorbate 60 was added to the nanoparticles (SLN3). While addition of polysorbate 60 significantly improved doxorubicin entrapment in SLN3 when compared to SLN2, the entrapment efficiency was ~35% (Table 1), which was too low to justify their use in subsequent studies. Therefore, alternate neutral nanoparticles (SLN4) composed of stearyl alcohol, Brij® 78 and vitamin E TPGS at a ratio of 1:1.2:1.6 was prepared (Table 1). The effect of sonication time during the preparation of SLN4 on doxorubicin entrapment and particle size is given in Table 1. With SLN4, it was possible to achieve >90% entrapment efficiency. The size of these nanoparticles, however, significantly increased over 3 days of storage (Fig. 1). Nanoparticles that were sonicated for a longer time were also less stable than those prepared without sonication.

Table 3B
Effect of complex processing conditions on the yield size. Effect of centrifugation speed on doxorubicin recovery as ion pair complex after 90 min of centrifugation. The data reported are mean ± standard deviation of $n = 3$ replicates.

Centrifugation speed (rpm)	% Dox complexed
1750 (417 × *g*)	12.0 ± 2.0
2500 (852 × *g*)	41.0 ± 0.5
3250 (1439 × *g*)	53.5 ± 1.1
4000 (2180 × *g*)	72.0 ± 0.8
4750 (3075 × *g*)	87.2 ± 0.1

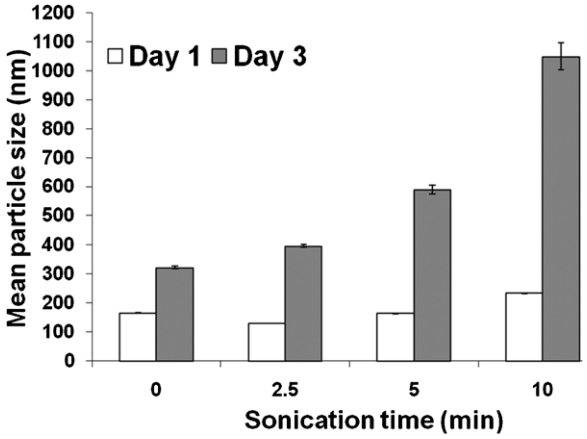

Fig. 1. Three-day stability of SLN4 at controlled room temperature as a function of sonication time during SLN preparation. ANOVA on particle size data obtained after three days showed that particle size at sonication time 0, 2.5, 5, and 10 min were significantly different (p-value <0.0001). The data reported are mean ± standard deviation of $n = 3$ replicates.

3.3. Lyophilization of SLN4

In order to stabilize SLN4, the formulation was lyophilized. Mono and disaccharides were added as cryoprotectants at a final concentration of 1%, 2.5%, 5%, 10%, and 20% (w/v). Dispersions were frozen at −80 °C for 3 days, and then rapidly transferred to lyophilization trays. The temperature of the condenser was reduced to −55 °C to minimize liquefaction of the frozen mass during freeze-drying. Dispersions in which trehalose, sucrose, and mannose were used produced a fluffy, light, and readily soluble lyophilized mass and were therefore selected for subsequent reconstitution and particle size analysis (Fig. 2). The mean particle size of the reconstituted lyophilized powders produced with trehalose, mannitol and sucrose were significantly different ($p < 0.0001$). The particle size of the reconstituted SLN4 was found to decrease with increasing cryoprotectant concentration. The most significant decrease was observed when the concentration of the cryoprotectants increased from 1% to 2.5% (w/v). Among the cryoprotectants, mannitol was found to stabilize SLN4 more than either trehalose or sucrose. At

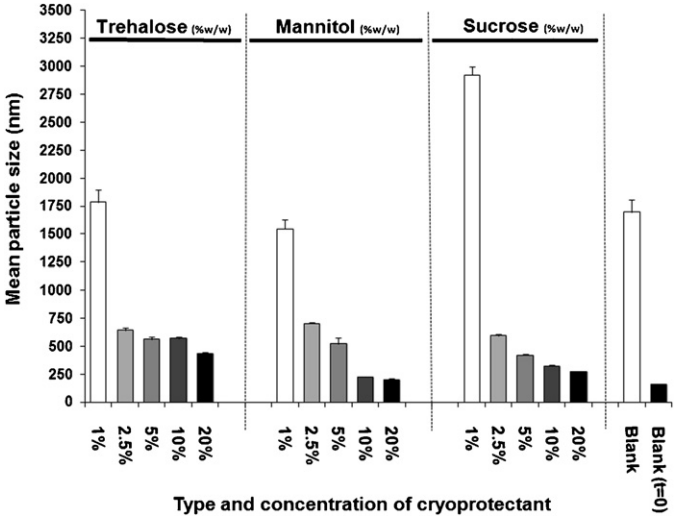

Fig. 2. Mean particle size of freeze dried SLN4 in the presence or absence of trehalose, mannitol or sucrose as cryoprotectant. Samples pre-frozen at −80 °C for 24 h were freeze dried at −55 °C and a pressure 1.65 Torr for 20 h (Labconco Freeze Zone 6). Freeze-dried samples were then redispersed in water to measure particle size. The data reported are mean ± standard deviation of $n = 3$ replicates.

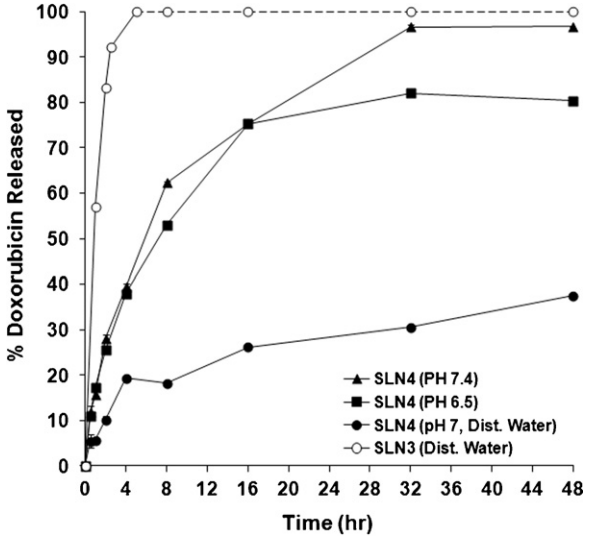

Fig. 3. Doxorubicin release from the SLN using dialysis tubing method. Drug release was evaluated in water, and in phosphate buffer at pH 6.8 and 7.4, representing the pH of the tumor and of blood, respectively. The data reported are mean ± standard deviation of $n = 3$ replicates.

10% (w/w) concentration, the size of the reconstituted SLN4 in trehalose, mannitol, and sucrose was 571.3, 226.8, and 322.6 nm, respectively. SLN4 dispersions without cryoprotectant produced a lyophilized cake that upon reconstitution in water resulted in 1700 nm particles, which were at least 10 fold larger than the size of the nanoparticles when freshly prepared.

3.4. In vitro drug release study

In vitro drug release studies were carried out by the dialysis method in different release media. After 4 h, 96% of doxorubicin was released from SLN3, which was dialyzed in plain water, whereas only 38%, 39%, and 19% of doxorubicin was released after 4 h from SLN4 at pH 6.8, 7.4 or distilled water, respectively (Fig. 3). Doxorubicin release from SLN4 followed a biphasic pattern characterized by an initial burst release followed by a plateau.

3.5. In vitro cell viability assay

The specific and non-specific toxicity of free doxorubicin in solution, doxorubicin loaded SLN4, and drug-free SLN4 against NCI/ADR-RES was investigated with an *in vitro* cell viability assay (Figs. 4 and 5). While free doxorubicin and drug-free SLN had marginal effect on the viability of the cells, doxorubicin loaded SLN4 had a significant and concentration–dependent effect on cell viability over a range from 0.1 to 5 μM. When cells were concurrently treated with 5 μM doxorubicin loaded SLN4 and SLN loaded with 100 nM MBO-asGCS, a significant decrease in cell viability was observed when compared with cells treated with doxorubicin loaded SLN4 only (Fig. 5).

4. Discussion

The objective of the present study was to ascertain whether the effectiveness of doxorubicin loaded into SLN against adriamycin-resistant NCI/ADR-RES cells could be augmented through concurrent treatment with MBO-asGCS loaded SLN. In order to achieve this objective, a water insoluble DTC-Dox ion-pair complex, with maximum yield at deoxytaurocholate to doxorubicin molar ratio of 3:1, was first prepared. Elemental analysis of the complex showed that the molecular ratio in the complex was 1:1 deoxytaurocholate

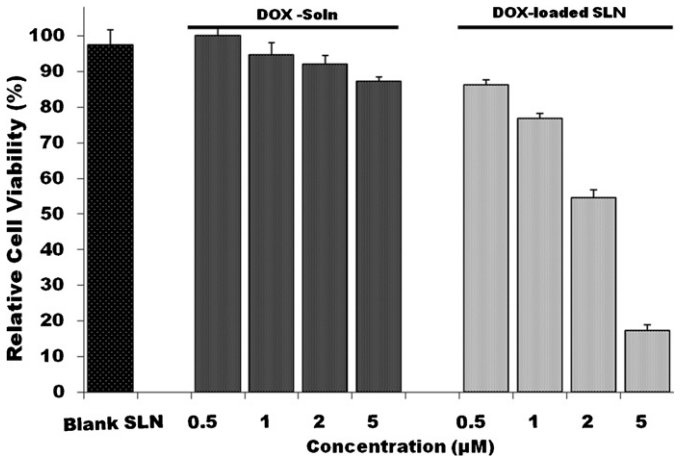

Fig. 4. Anticancer effect of doxorubicin solution, doxorubicin hydrophobic complex loaded SLN4, and drug-free SLN4 on adriamycin-resistant NCI/ADR-RES human ovary cancer cells. Viable cell number was ascertained by measuring luminescent ATP using CellTiter-Glo® reagent. Vertical bars indicate the mean cell count +SEM ($n = 6$).

to doxorubicin. The complex did not dissolve in water or in highly nonpolar solvents (*e.g.*, chloroform, dichloromethane, *n*-hexane) however, it was slightly soluble in alcohols (methyl alcohol, ethyl alcohol and isopropyl alcohol).

Poor entrapment of the DTC-Dox ion-pair in SLN1 and SLN2 during SLN preparation could partially be attributed to sonication, which may have caused the ion-pairing to dissociate leading to the release of soluble doxorubicin salt into the aqueous media. To enhance doxorubicin entrapment and reduce SLN size, CTAB concentration was reduced by 50% and substituted with polysorbate 60 (SLN3) to confer steric and electrostatic stability to the particles. The mean particle size of SLN3 was 139 nm with a doxorubicin entrapment of 33%, which was an improvement over SLN2 for which doxorubicin entrapment was less than 5%. These results

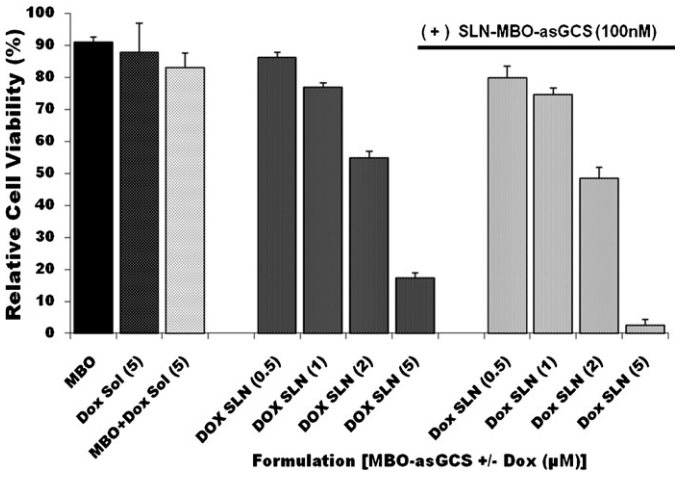

Fig. 5. Anticancer effect of doxorubicin solution, doxorubicin hydrophobic complex-loaded SLN4, and concurrent treatment with SLN-MBOasGCS (100 nM) and doxorubicin-complex-loaded SLN4 on adriamycin-resistant NCI/ADR-RES human ovary cancer cells. Viable cell number was determined by measuring luminescent ATP using CellTiter-Glo® reagent. Vertical bars indicate the mean cell count +SEM ($n = 6$). C: negative control; MBO: mixed backbone antisense glucosyceramide synthase oligonucleotide; Dox: Doxorubicin; Dox SLN: Solid lipid nanoparticles loaded with hydrophobic doxorubicin complex; Dox Sol: Doxorubicin solution; (+) SLN-MBO-asGCS: indicates concurrent treatment of two SLN *i.e.*, SLN4 (containing doxorubicin ion pair complex), and SLN2 MBO-asGCS (ceramide based SLN loaded with MBO-asGCS); the number in the parentheses against the formulations in the *X*-axis represent concentration of treatment in μM.

Table 4
The mechanism of doxorubicin release from SLN as estimated from the R^2 value for each kinetic model corresponding to the *in vitro* release data obtained.

	Dissolution media [R^2 (n)]		
Model	pH 7.4	pH 6.8	Water
Zero order	0.863	0.819	0.785
First order	0.987	0.920	0.817
Higuchi Model	0.972	0.950	0.913
Hixon Crowell	0.983	0.891	0.807
Korsmeyer–Pappas	0.980 (0.52)	0.981 (0.49)	0.932 (0.45)

suggested that the presence of CTAB in nanoparticles limited its ability to accommodate the DTC-Dox ion-pair complex. More likely the positively charged CTAB competes with the positively charged (protonated) doxorubicin for incorporation into the particles. The observed 93% doxorubicin release in 2.5 h for SLN3 in water (Fig. 3), suggested that the ion-pair complex was either dissociated upon particle formation or remained trapped in the static water layer formed by polysorbate 60 around the particles. Due to the dissociation of the ion-pair complex and the fast release of doxorubicin, two separate SLN were prepared; one carrying doxorubicin (SLN4) and the other loaded with MBO-asGCS. SLN4 was prepared with the main objective of enhancing doxorubicin entrapment in SLN. In SLN4, cationic CTAB was substituted with the neutral surfactants: Vitamin E TPGS and Brij® 78. A similar surfactant and cosurfactant combination was shown by Ma et al. (2009) to efficiently entrap doxorubicin. While doxorubicin entrapment was significantly improved in comparison to its entrapment in SLN containing CTAB or CTAB/polysorbate, SLN4 proved to be unstable in water, exhibiting significant increases in particle size with time, which was proportional to the sonication time used during SLN preparation. To stabilize SLN4, it was freeze-dried. Trehalose, mannitol and sucrose were selected as cryoprotectant. The original size of the nanoparticle was maintained when 20% (w/v) cryoprotectant solutions were used. No differences in drug entrapment efficiencies before and after the lyophilization were observed.

In dissolution media, SLN4 formulation exhibited a biphasic release profile: an initial burst followed by a plateau, with low, intermediate and high rates, in water and in pH 6.8 and pH 7.4 phosphate buffers, respectively (Fig. 3). These results demonstrated the role of counterions, for example phosphate ion, in facilitating the doxorubicin release from its complex in the nanoparticles. In order to further elucidate the mechanism of drug release, *in vitro* data were fitted into various drug release models (Table 4). Both Higuchi and Korsmeyer–Pappas models were found to describes the maximum variability in data ($R^2 > 90\%$). The exponent value (n) in the Korsmeyer–Pappas model for doxorubicin release in water and in pH 7.4 and 6.8 media was approximately 0.45. Thereby, it could be concluded that fickian diffusion is the rate controlling step in doxorubicin release from the SLN (Korsmeyer et al., 1983), which was confirmed by the linearity of the release data when applying the Higuchi square root of time model. Consequently, if we hypothesize that the DTC-Dox ion-pair complex is heterogeneously distributed in the lipid matrix, the release of doxorubicin into the media would be faster for the complex present at the surface of the SLN than those in the core because of the differences in diffusion path lengths. Similar drug release patterns were suggested by Wong et al. (2004) who monitored the release of doxorubicin from nanoparticles loaded with doxorubicin/dextran sulfate complexes. Overall, the results obtained in this study suggest that the entrapped complex reduced the availability of free doxorubicin in water, in spite of the effect of counterions in the media on facilitating drug release. When taking into consideration the small size of the complex-loaded SLN, which would enhance its permeability around the leaky tumor vasculature, and the small percentage

of doxorubicin leaking during circulation (25% in 2 h), an increase in the bioavailability of the drug at target size would be expected (Wang and Thanou, 2010).

In vitro cell viability studies were subsequently carried out to delineate the efficacy of doxorubicin-loaded nanoparticle over free doxorubicin against adriamycin resistant cancer cells (Fig. 4). NCI/ADRRes cells were treated with either free doxorubicin in solution or DTC-Dox ion complex loaded in nanoparticles (SLN4). Whereas free doxorubicin in solution did not have a significant effect on the cells because more than 80% of the cells were viable at the end of the experiment, DTC-Dox ion complex loaded SLN4 demonstrated enhanced and dose-dependent reduction in cell survival, presumably due to the increased delivery of doxorubicin to the cells. Enhanced intracellular doxorubicin availability due to the ability of doxorubicin loaded SLN to by-pass P-gp efflux transported was reported by Dong et al. (2009). Furthermore, formulation ingredients, such as vitamin E TPGS and Brij® 78, were also shown to chemosensitize resistant cancer cells by fluidizing the cell membrane, and/or depleting ATP, and/or inhibiting drug efflux, and/or reducing glutathione/glutathione *S*-transferase detoxification activity (Dong et al., 2009; Dumortier et al., 2006; Ma et al., 2009; Wong et al., 2006b,c).

At cytoplasmic level, upregulated conversion of ceramide to glucosylceramide by glucosylceramide synthase (GCS) was found to be associated with increased levels of P-gp expression, as previously noted. Down-regulating GCS using an MBO was shown to sensitize NCI/ADR-RES cells to doxorubicin by increasing ceramide levels, which subsequently leads to cell apoptosis (Liu et al., 2008). This effect was more pronounced when the MBO-asGCS was delivered by SLN (Siddiqui et al., 2010). A further dose-dependent decrease in cell viability was observed when the cells were concurrently treated with doxorubicin-loaded into SLN4 and SLN loaded with MBO-asGCS (Fig. 5).

5. Conclusion

In conclusion, the formation of lipophilic doxorubicin-ion pair complex is essential for inclusion into lipid-based nanoparticles. The nature of SLN determines doxorubicin entrapment efficiency with positively charged SLN showing lower entrapment efficiency than the neutral SLN. While the cationic nanoparticle induced the dissociation of the ion pair complex as observed by the fast doxorubicin release in water, a slow release was attained in neutral nanoparticles. Less than <40% of doxorubicin was released in 32 h from the neutral SLN4 nanoparticles in water. In phosphate buffer, however, close to 80% of doxorubicin was released within 16 h, which could be attributed to the effect of ions on the dissociation of the ion pair complex. Entrapment of doxorubicin in nanoparticle was also shown to enhance the efficacy of doxorubicin against adriamycin resistant cancer cells. The concurrent treatment of cells with SLN loaded with MBO-asGCS and SLN4 loaded with doxorubicin was also shown to significantly reduce cell viability, which suggested that SLN is an efficient non-viral carrier for the cellular delivery of chemotherapeutics and MBOs. This study further provided the proof-of-concept that SLN-facilitated MBO-asGCS delivery down-regulates GCS and consequently sensitizes the NCI/ADR-RES cells to doxorubicin. However, a number of details concerning the uptake and intracellular trafficking of SLN4 and SLN loaded with MBO-asGCS remain unknown, and warrant further investigation.

Acknowledgment

This work was partially supported by the United State Public Health Service/NIH grant P20 RR16456 from the National Center of Research Resources (Y.Y.L).

References

Bacso, Z., Nagy, H., Goda, K., Bene, L., Fenyvesi, F., Matkó, J., Szabó, G., 2004. Raft and cytoskeleton associations of an ABC transporter: P-glycoprotein. Cytometry Part A 61A, 105–116.
Cabot, M.C., Giuliano, A.E., Han, T.Y., Liu, Y.Y., 1999. SDZ PSC 833, the cyclosporine A analogue and multidrug resistance modulator, activates ceramide synthesis and increases vinblastine sensitivity in drug-sensitive and drug-resistant cancer cells. Cancer Res. 59, 880–885.
Choi, C.H., 2005. ABC transporters as multidrug resistance mechanisms and the development of chemosensitizers for their reversal. Cancer Cell Int. 5.
Dong, X., Mattingly, C.A., Tseng, M.T., Cho, M.J., Liu, Y., Adams, V.R., Mumper, R.J., 2009. Doxorubicin and paclitaxel-loaded lipid-based nanoparticles overcome multidrug resistance by inhibiting P-glycoprotein and depleting ATP. Cancer Res. 69, 3918–3926.
Dumortier, G., Grossiord, J.L., Agnely, F., Chaumeil, J.C., 2006. A review of poloxamer 407 pharmaceutical and pharmacological characteristics. Pharm. Res. 23, 2709–2728.
Gottesman, M.M., 2002. Mechanisms of cancer drug resistance. Annu. Rev. Med. 53, 615–627.
Gouaze-Andersson, V., Cabot, M.C., 2006a. Glycosphingolipids and drug resistance. Biochim. Et. Biophys. Acta (BBA): Biomembr. 1758, 2096–2103.
Gouaze-Andersson, V., Cabot, M.C., 2006b. Glycosphingolipids and drug resistance. Biochim. Biophys. Acta 1758, 2096–2103.
Gouaze, V., Liu, Y.Y., Prickett, C.S., Yu, J.Y., Giuliano, A.E., Cabot, M.C., 2005. Glucosylceramide synthase blockade down-regulates P-glycoprotein and resensitizes multidrug-resistant breast cancer cells to anticancer drugs. Cancer Res. 65, 3861–3867.
Gouaze, V., Yu, J.Y., Bleicher, R.J., Han, T.Y., Liu, Y.Y., Wang, H., Gottesman, M.M., Bitterman, A., Giuliano, A.E., Cabot, M.C., 2004. Overexpression of glucosylceramide synthase and P-glycoprotein in cancer cells selected for resistance to natural product chemotherapy. Mol. Cancer Ther. 3, 633–639.
Korsmeyer, R.W., Gurny, R., Doelker, E., Buri, P., Peppas, N.A., 1983. Mechanisms of solute release from porous hydrophilic polymers. Int. J. Pharm. 15, 25–35.
Li, Y.C., Park, M.J., Ye, S.K., Kim, C.W., Kim, Y.N., 2006. Elevated levels of cholesterol-rich lipid rafts in cancer cells are correlated with apoptosis sensitivity induced by cholesterol-depleting agents. Am. J. Pathol. 168, 1107–1118 (quiz 1404–1105).
Liu, Y.Y., Gupta, V., Patwardhan, G.A., Bhinge, K., Zhao, Y., Bao, J., Mehendale, H., Cabot, M.C., Li, Y.T., Jazwinski, S.M., 2010. Glucosylceramide synthase upregulates MDR1 expression in the regulation of cancer drug resistance through cSrc and beta-catenin signaling. Mol. Cancer 9, 145.
Liu, Y.Y., Han, T.Y., Giuliano, A.E., Cabot, M.C., 1999. Expression of glucosylceramide synthase, converting ceramide to glucosylceramide, confers adriamycin resistance in human breast cancer cells. J. Biol. Chem. 274, 1140–1146.
Liu, Y.Y., Han, T.Y., Giuliano, A.E., Cabot, M.C., 2001. Ceramide glycosylation potentiates cellular multidrug resistance. FASEB J. 15, 719–730.
Liu, Y.Y., Han, T.Y., Giuliano, A.E., Hansen, N., Cabot, M.C., 2000. Uncoupling ceramide glycosylation by transfection of glucosylceramide synthase antisense reverses adriamycin resistance. J. Biol. Chem. 275, 7138–7143.
Liu, Y.Y., Han, T.Y., Yu, J.Y., Bitterman, A., Le, A., Giuliano, A.E., et al., 2004. Oligonucleotides blocking glucosylceramide synthase expression selectively reverse drug resistance in cancer cells. J. Lipid Res. 45, 933–940.
Liu, Y.Y, Yu, J.Y., Yin, D., Patwardhan, G.A., Gupta, V., Hirabayashi, Y., Holleran, W.M., Giuliano, A.E., Jazwinski, S.M., Gouaze-Andersson, V., Consoli, D.P., Cabot, M.C., 2008. A role for ceramide in driving cancer cell resistance to doxorubicin. FASEB J. 22, 2541–2551.
Lucci, A., Han, T.Y., Liu, Y.Y., Giuliano, A.E., Cabot, M.C., 1999. Multidrug resistance modulators and doxorubicin synergize to elevate ceramide levels and elicit apoptosis in drug-resistant cancer cells. Cancer 86, 300–311.
Ma, P., Dong, X., Swadley, C.L., Gupte, A., Leggas, M., Ledebur, H.C., Mumper, R.J., 2009. Development of idarubicin and doxorubicin solid lipid nanoparticles to overcome Pgp-mediated multiple drug resistance in leukemia. J. Biomed. Nanotechnol. 5, 151–161.
Müller, R.H., Mäder, K., Gohla, S., 2000. Solid lipid nanoparticles (SLN) for controlled drug delivery – a review of the state of the art. Eur. J. Pharm. Biopharm. 50, 161–177.
Norris-Cervetto, E., Callaghan, R., Platt, F.M., Dwek, R.A., Butters, T.D., 2004. Inhibition of glucosylceramide synthase does not reverse drug resistance in cancer cells. J. Biol. Chem. 279, 40412–40418.
Patwardhan, G.A., Zhang, Q.J., Yin, D., Gupta, V., Bao, J., Senkal, C.E., Ogretmen, B., Cabot, M.C., Shah, G.V., Sylvester, P.W., Jazwinski, S.M., Liu, Y.Y., 2009. A new mixed-backbone oligonucleotide against glucosylceramide synthase sensitizes multidrug-resistant tumors to apoptosis. PLoS ONE 4, e6938.
Pérez-Sayáns, M., Somoza-Martín, J.M., Barros-Angueira, F., Diz, P.G., Rey, J.M.G., García-García, A., 2010. Multidrug resistance in oral squamous cell carcinoma: the role of vacuolar ATPases. Cancer Lett. 295, 135–143.
Saltiel, E., McGuire, W., 1983. Doxorubicin (adriamycin) cardiomyopathy. West J. Med. 139, 332–341.
Siddiqui, A., Patwardhan, G.A., Liu, Y.Y., Nazzal, S., 2010. Mixed backbone antisense glucosylceramide synthase oligonucleotide (MBO-asGCS) loaded solid lipid nanoparticles *in vitro* characterization and reversal of multidrug resistance in NCI/ADR-RES cells. Int. J. Pharm. 400, 251–259.

van Den Elsen, J.M., Kuntz, D.A., Hoedemaeker, F.J., Rose, D.R., 1999. Antibody C219 recognizes an alpha-helical epitope on P-glycoprotein. Proc. Natl. Acad. Sci. U.S.A. 96, 13679–13684.

van Meer, G., Wolthoorn, J., Degroote, S., 2003. The fate and function of glycosphingolipid glucosylceramide. Philos. Trans. R. Soc. Lond. B Biol. Sci. 358, 869–873.

Wang, M., Thanou, M., 2010. Targeting nanoparticles to cancer. Pharmacol. Res. 62, 90–99.

Wong, H.L., Bendayan, R., Rauth, A.M., Li, Y., Wu, X.Y., 2007. Chemotherapy with anticancer drugs encapsulated in solid lipid nanoparticles. Adv. Drug Deliv. Rev. 59, 491–504.

Wong, H.L., Bendayan, R., Rauth, A.M., Wu, X.Y., 2004. Development of solid lipid nanoparticles containing ionically complexed chemotherapeutic drugs and chemosensitizers. J. Pharm. Sci. 93, 1993–2008.

Wong, H.L., Bendayan, R., Rauth, A.M., Wu, X.Y., 2006a. Simultaneous delivery of doxorubicin and GG918 (Elacridar) by new polymer-lipid hybrid nanoparticles (PLN) for enhanced treatment of multidrug-resistant breast cancer. J. Control. Release 116, 275–284.

Wong, H.L., Bendayan, R., Rauth, A.M., Xue, H.Y., Babakhanian, K., Wu, X.Y., 2006b. A mechanistic study of enhanced doxorubicin uptake and retention in multidrug resistant breast cancer cells using a polymer-lipid hybrid nanoparticle system. J. Pharmacol. Exp. Ther. 317, 1372–1381.

Wong, H.L., Rauth, A.M., Bendayan, R., Manias, J.L., Ramaswamy, M., Liu, Z., Erhan, S.Z., Wu, X.Y., 2006c. A new polymer-lipid hybrid nanoparticle system increases cytotoxicity of doxorubicin against multidrug-resistant human breast cancer cells. Pharm. Res. 23, 1574–1585.

Ye, S., MacEachran, D.P., Hamilton, J.W., O'Toole, G.A., Stanton, B.A., 2008. Chemotoxicity of doxorubicin and surface expression of P-glycoprotein (MDR1) is regulated by the Pseudomonas aeruginosa toxin Cif. Am. J. Physiol. Cell Physiol. 295, C807–C818.